A R C H I V E S O F M E T A L L U R G Y A N D M A T E R I A L S
Volume 50 2005 Issue 4

I. STANIEWSKI*, W. DERDA*

APPLICATION OF THE CFD COMPUTING TECHNIQUE TO NUMERICAL MODELING OF CONTINUOUS CASTING OF STEEL

ZASTOSOWANIE OBLICZENIOWYCH TECHNIK CFD DO MODELOWANIA NUMERYCZNEGO PROCESU CIĄGŁEGO ODLEWANIA STALI

The paper present the results of simulation of the process of steel solidification in the casting mould zone with the use of the CFD technique and the FLUENT® program. The solution of the $k-\varepsilon$ mathematical model of turbulence based on a system of differential equations of the conservation of mass, momentum and energy was obtained, thanks to which it was possible to make a map of the distribution of liquid steel velocity fields, temperature variations, as well as the crystallization front in a solidifying square cross-section continuous slab. The computation results made it possible to optimize the topology of the grid (the number of control volumes) in order to map it over the whole object.

W pracy przedstawiono wyniki symulacji procesu krzepnięcia stali w strefie krystalizatora, z wykorzystaniem techniki CFD i programu FLUENT®. Uzyskano rozwiązanie układu równań zastosowanego matematycznego modelu turbulencji $k-\varepsilon$ opartego na układzie równań różniczkowych zachowania masy, pędu i energii, dzięki któremu możliwym było sporządzenie mapy rozkładu pól prędkości ciekłej stali, zmian przebiegu temperatur, a także frontu krystalizacji w krzepnącym wlewku ciągłym o przekroju kwadratowym. Wyniki obliczeń pozwoliły zoptymalizować topologię siatki (liczbę objętości kontrolnych), aby odwzorować ją na całym obiekcie.

Nomenclature

T_L — liquidus temperature, (K)
T_S — solidus temperature, (K)
T — temperature, (K)
h_{ref} — reference (standard) enthalpy ($J \cdot kg^{-1}$)
c_p — specific heat at the constant pressure, ($J \cdot kg^{-1} \cdot K^{-1}$)

* WYDZIAŁ INŻYNIERII PROCESOWEJ, MATERIAŁOWEJ I FIZYKI STOSOWANEJ, POLITECHNIKA CZĘSTOCHOWSKA, 42-200 CZĘSTOCHOWA, AL. ARMII KRAJOWEJ 19

T_{ref} — reference (standard) temperature, (K)
H_L — latent heat of phase transition (solidification), ($J \cdot kg^{-1}$)
H — enthalpy of steel, ($J \cdot kg^{-1}$)
$\vec{v}$ — liquid steel velocity, ($m \cdot s^{-1}$)
S — heat source ($J \cdot kg^{-1} \cdot K^{-1}$)
k — thermal conductivity, ($W \cdot m^{-1} \cdot K^{-1}$)
μ — viscosity ($kg \cdot m^{-1} \cdot s^{-1}$)
ρ_0 — flux density (constant)
β — coefficient of thermal expansion
z — distance from the meniscus level, (m)
U_o — casting speed, ($m \cdot s^{-1}$)

1. Introduction

A continuous pursuit of the improvement of the quality of continuous slabs and the wish for solving ongoing production problems concerning individual continuous casting installations are accomplished through a number of studies aimed at increasing casting speed and improving the already existing steelmaking technologies. A characteristic feature of modern technologies is an increasingly common use of integrated continuous casting and rolling. As a result of such a combination of processes, considerable energy savings and a high-quality final product are gained. Because of the complexity of phenomena occurring during continuous steel casting, and particularly during solidification, numerical simulations of partial processes are appropriate and convenient tools for the assessment of accuracy of a technology being implemented, the prediction of the properties of continuous slabs and the explanation of the causes of occurring any defects. The input of such computations to the extension of existing databases concerning this modern and constantly developed branch of metallurgy is also important. The mathematical modeling of heat exchange processes and the behaviour of nonmetallic inclusions in the liquid phase, and the understanding of the effect of electromagnetic stirring on the process of liquid steel solidification in the casting mould are problems that are still topical and continuously studied [1-9]. The subject of numerous publications are the results of numerical computations carried out using computational codes, such as CFX [10-12], PHOENICS [13], ELECTRA [14], CFD [15-18], FORTRAN [19, 20], FIDAP [21].

The present paper provides the results of simulation of the process of steel solidification in the casting mould zone, while considering the transfer of mass, momentum and energy, with the use of the CFD technique and the FLUENT® program. The current development of CFD techniques and a systematic increase in the capacity of computing units (computers) facilitates conducting of studies involving the modeling of ever complex problems associated with solidification, with phase and thermal changes occurring at this stage of the continuous steel casting process. The computations were

performed using real data concerning an industrial facility — a 6-strand radial-type COS installation casting square cross-section slabs.

2. Scope of investigation

The purpose of model investigation carried out was to make maps of velocity and temperature fields and the relative position of the liquid and solid phases in the square cross-section continuous slab in the continuous casting process with limitation to the casting mould zone.

Numerical computation was carried out for conditions corresponding to the casting of steel 18G2A (St52-3 acc. to DIN, E355-CC acc. to ISO) on strand no. 6 of the COS plant using an submerged entry nozzle, without allowing for electromagnetic stirring, with a variable behaviour of heat exchange on the continuous slab walls. The average chemical composition of the steel for which the computation was performed is given in Table 1.

TABLE 1

Average chemical composition of steel 18G2A, wt %

Contents of elements, wt %										
[C]	[Mn]	[Si]	[P]	[S]	[Cr]	[Ni]	[Cu]	[Al]	[Mo]	[Sn]
0.190	1.373	0.287	0.020	0.010	0.053	0.067	0.193	0.023	0.0147	0.0123

3. The object of computation

The object of computation was a 1 m-long radial-shaped mould after modernization of the 6- strands COS installation of an radius of $R = 7$ m, serving for casting of 160 mm-side square cross-section slabs. Preliminary numerical computations were carried out for half of the casting mould (test object) on account of its symmetry in relation to the vertical plane passing through the centre of the tundish entry nozzle and the geometrical centre of the casting mould cross-section. The scope of computation on the test object covered a 0.78 m-long mould before modernization and filling it with liquid steel by the open stream method with a tundish entry nozzle diameter of $d = 16$ mm. For the investigation objective set, one of the main problems was to determine the correct topology of the discretized computational grid and to define, correctly and appropriately to the real conditions, the boundary conditions for the slab walls in respect of heat exchange. In the first stage, computation was performed for the grid condensed in the casting mould inlet zone, and then, in the second stage, the number of nodes along the object's walls was increased, thus considerably increasing the total number of control volumes. All computational variants used are shown in Table 2.

TABLE 2

Variants of computer modeling for the test object

No.	Number of nodes along the slab wall	Sum of control volumes
1	100*)	121000
2	100	121000
3	120	169200
4	150	211500
5	200	242000
6	300	423000

Note: *) The grid is condensed in the liquid steel filling zone

Proportionally to the number of control volumes the computation time increased, with the computation being conducted with a time step from 0.001 to 0.01 s. After modifying the computational grid topology due to adopting a new geometry of the object, numerical computation was carried out for casting steel according to the technology using a submerged entry nozzle.

4. Mathematical model

The $k - \varepsilon$ mathematical model of turbulence based on the system of differential equations of the conservation of mass, momentum and energy (the Navier-Stokes equation) was employed, allowing for the equations of the phase change occurring in the temperature range of $T_L \leftrightarrow T_S$, which is associated with the thermal effect ($0 < \Delta H < H_L$), where the liquid phase fraction f varies from 0 to 1 [22]:

$$f = \begin{cases} 0 \Rightarrow T < T_S \\ \frac{T-T_S}{T_L-T_S} \Rightarrow T_S \leqslant T \leqslant T_L \\ 1 \Rightarrow T > T_L \end{cases} . \quad (1)$$

While, the total enthalpy of steel in the energy equation is described by the relationship:

$$H = h + \Delta H, \quad (2)$$

where:

$$h = h_{ref} + \int_{T_{ref}}^{T} c_p dT \quad (3)$$

$$\Delta H = f \cdot H_L. \quad (4)$$

For the liquid↔solid phase change, the equation of energy is described according to [23]:

$$\frac{\partial}{\partial t}(\rho H) + \nabla \cdot \left(\rho \vec{v} H\right) = \nabla \cdot (k \nabla T) + S, \tag{5}$$

where:

$$S = -\partial H \frac{\partial f}{\partial T}. \tag{6}$$

The Heat Source Method with the rational simplification of the mathematical model in the form of a constant thermal conductivity, $k = 34\mathrm{W} \cdot \mathrm{m}^{-1} \cdot \mathrm{K}^{-1}$ for both phases (liquid and solid) was employed. The solution for the temperature parameter is iteration between the energy equation (5) and the liquid phase change equation (1). Due to the occurrence of the semi-liquid phase, regarded in this case as a porous phase, the following expressions have been added to the differential equations of momentum and turbulence energy for the sources [24] of:

momentum
$$S = \frac{(1-f)^2}{(f^3 + \epsilon)} A_{mush} \left(\vec{U} - \vec{U_o}\right) \tag{7}$$

and turbulence
$$S = \frac{(1-f)^2}{(f^3 + \epsilon)} A_{mush} \phi \tag{8}$$

where :
$$A_{mush} = \frac{\mu \cdot 180}{d_d^2}, \tag{9}$$

d_d — dendrite size (taken as $\cong 100\mu$m acc. to [24]), U_o — casting speed (taken as 0.04 $\mathrm{m \cdot s^{-1}}$, as the average value for the test object), ϕ — magnitudes to be found (k, ε), ϵ — a sufficiently small number for avoiding division by zero (taken as = 0.001).
The variation of liquid steel density is described by the Boussinesq model used for many natural convection fluxes, for which the convergence of iterative computations can be reached faster than by configuring the problem of solidification with the liquid steel density as a function of temperature. This model assumes the density to be a constant value in all equations solved, except for the expression concerning the hydrostatic lift in the angular momentum equation [24]:

$$(\rho - \rho_0)\, g \approx -\rho_0 \beta (T - T_0)\, g. \tag{10}$$

The solution of equation (10) will be obtained by applying the Boussinesq approximation, $\rho = \rho_0 (1 - \beta \Delta T)$, to eliminate the density ρ from the expression for the hydrostatic lift. This approximation is accurate for small changes in density, when $\beta (T - T_0) << 1$.

5. Boundary conditions

When analyzing the process of solidification of steel 18G2A under industrial conditions and the technology of casting of this steel grade, the temperatures T_L, T_S were determined from the relationships provided by the authors of work [25]:

$$T_L = 1537 - 88(\%C) - 25(\%S) - 5(\%Cu) - 8(\%Si) - 5\%(Mn) - 2(\%Mo) \\ -4(\%Ni) - 1.5(\%Cr) - 18(\%Ti) - 2(\%V) - 30(\%P) \tag{11}$$

$$T_S = 1535 - 200(\%C) - 12.5(\%Si) - 6.8(\%Mn) - 124.5(\%P) - 183.9\%(S) \\ -4.3(\%Ni) - 1.4(\%Cr) - 4.1(\%Al). \tag{12}$$

The degree of steel superheating, ΔT, defined as the difference between the actual temperature of casting of this steel grade and the temperature T_L, was determined from the measurement of temperature taken on the industrial facility, corresponding to the temperature of liquid steel at the $^1/_3$ of the height as measured from the liquid steel table in the tundish.

Following the concept of the authors of many works [22, 26-29], the computation concerning the test object was carried out for a present boundary condition on the casting mould walls in the form of a constant heat exchange coefficient, h, which obviously considerably simplified the way in which the computations were conducted, and particularly shortened their time. Literature provides various values of the coefficient h; in the present computation, the value of 2000 W/m^2·K was assumed. By varying the thermal conditions and trying to faithfully represent the character of heat exchange at the slab plane/casting mould wall interface, the boundary condition for the slab walls was modified. This modification consisted in the creation of an additional computational procedure, the so called UDF (User Defined Function) procedure, in the C++ environment on the subsequent stage of computation [30], supplementary to the existing Fluent program's procedures, with the aim of allowing for the complex boundary conditions. Then, the parameter of variable heat flux on the slab walls, $q_{steel/mold}$ [31], as proposed by J. Savage and W. H. Pritchard [30] and used elsewhere [32, 33], was introduced, which substantially changed the previous way of considering the process.

$$q_{steel/mold} = A - B\sqrt{\frac{z}{U_o}}. \tag{13}$$

The constants A and B are, respectively: A = 2680 kW/m^2, B = 335 kW/m^2·s$^{1/2}$ [32]. Some drawback resulting from the assumption of this condition is that it not very accurately describes the heat exchange in the upper casting mould zone — immediately below the meniscus. However, for the objective set, it was assumed in the process of computation that the accuracy of the characteristics of thermal conditions prevailing in

the real facility so obtained through the boundary condition used in this form would be sufficient. The remaining boundary conditions and casting mould parameters are given in Table 3.

TABLE 3

Summary of the values of parameters adopted in the model computation of the COS process for the whole facility

Description of parameter	Value	Unit
Casting mould / slab side, a	0.16	m
Tundish entry nozzle diameter, d	0.03	m
Height steel in mould (meniscus level), l	0.85	m
Casting speed, U_o	0.0325	$m \cdot s^{-1}$
Speed of steel pouring into the mould, U_w	1.176	$m \cdot s^{-1}$
Steel temperature (solidus), T_S	1479.25	°C
Steel temperature (liquidus), T_L	1508.65	°C
Steel superheating temperature, ΔT	41.6	°C
Ambient $T_{ot.}$	30	°C
Thermal conductivity, k	34	$W \cdot m^{-1} \cdot K^{-1}$
Coefficient of thermal expansion, β	0.0001	K^{-1}
Coefficient of dynamic viscosity, μ	0.007	$kg \cdot m^{-1} \cdot s^{-1}$
Latent heat of steel solidification, H_L	$2.7 \cdot 10^5$	$J \cdot kg^{-1}$
Specific heat, C_p	680	$J \cdot kg^{-1} \cdot K^{-1}$
Density of steel, ρ	7010	$kg \cdot m^{-3}$

The computation results for the test object are represented graphically in the form of the variation of temperature (Fig. 2) and velocity (Fig. 3) distributions for characteristic edges in the cross-section and longitudinal section of the continuous slab (Fig. 1).
On account of the grid topology, comparison of the variations of velocities and temperatures in the characteristic planes of the slab cross-section was made. The results obtained in Variant 1 have shown that condensing of the grid in the casting mould inlet zone has an unfavourable effect on computation accuracy — the obtained results clearly deviate from the others (Fig. 3).
It is noteworthy that the highest value of liquid steel stream temperature occurs almost in the mid-height of the casting mould working part (30 cm from the meniscus). This is also confirmed by the diagram of variation of liquid steel velocity shown in Fig. 3a. The curvilinear behaviour of variations of liquid steel stream velocity in the cross-section at the mid-height of the slab suggest the existence of dead zones (Fig. 3c). Indeed, it should be borne in mind that the performed computation concerns a system, where the metal motion caused by electromagnetic stirring of the liquid slab core has been neglected.

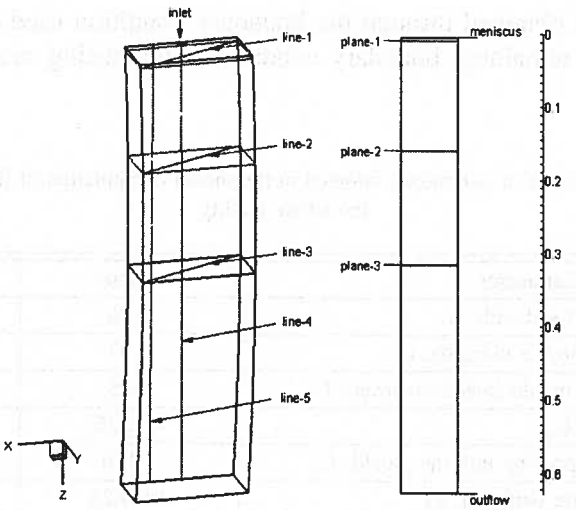

Fig. 1. Conceptual planes and edges (for computation result presentation)

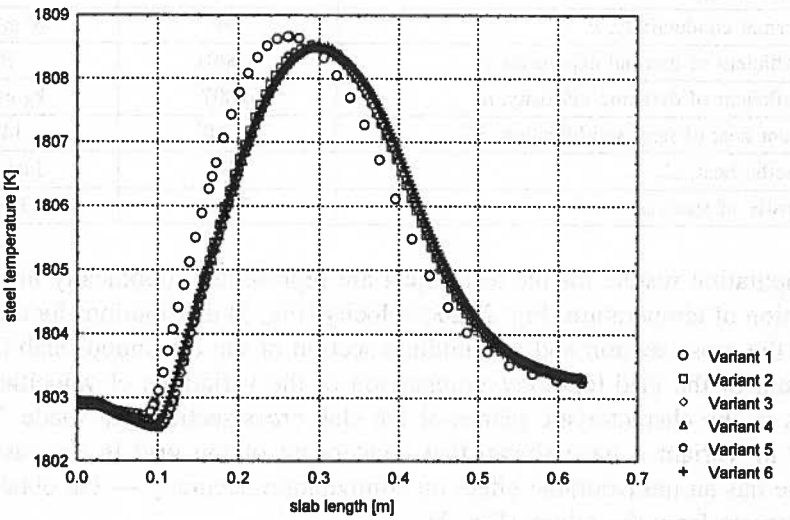

Fig. 2. Distribution of temperatures on the longitudinal section of the slab (line-5), Variants 1 — 6 acc. to Table 2

Moreover, the characteristics shown in Figures 2 and 3 indicate that the number of control volumes in the test object for Variant 4 can be regarded as optimal. Further increasing the number of control volumes does not significantly distort the numerical modeling results (particularly in zones more distant from the meniscus), while the computation time clearly increases. Thus, by maintaining the appropriate proportions in distances between the nodes along the walls (the number of control volumes for Variant 4) the mapping was made over the entire facility.

a)

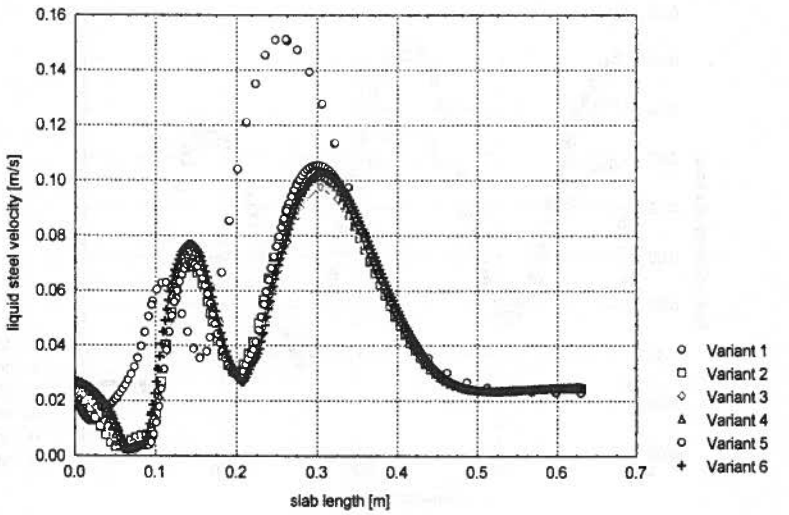
liquid steel velocity [m/s]
slab length [m]
Variant 1
Variant 2
Variant 3
Variant 4
Variant 5
Variant 6

b)

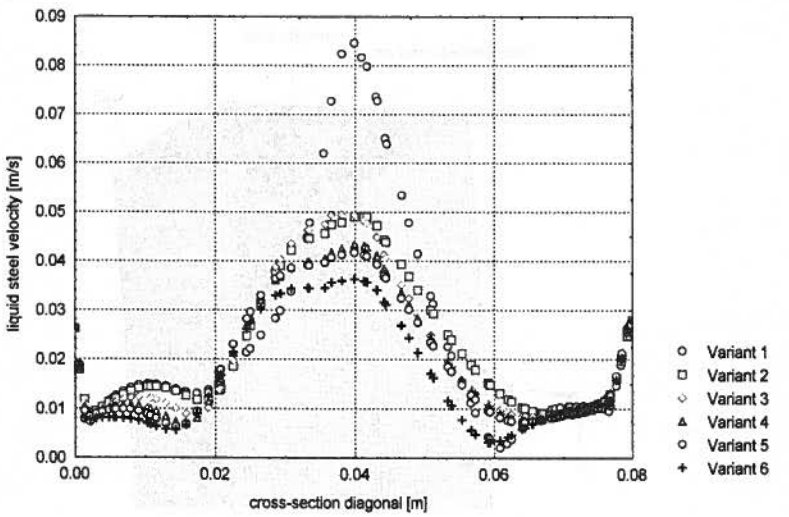
liquid steel velocity [m/s]
cross-section diagonal [m]
Variant 1
Variant 2
Variant 3
Variant 4
Variant 5
Variant 6

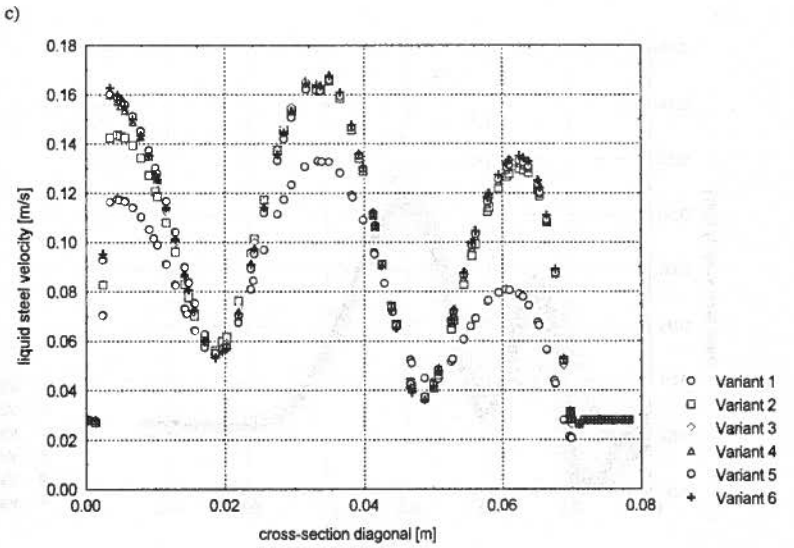

Fig. 3. Distribution of liquid steel velocities within the slab at the edges: a) 40 cm from the facility centre (line-5); b) 5 mm from the meniscus (line-1); c) at the $^1/_2$ of the casting height (line-3)

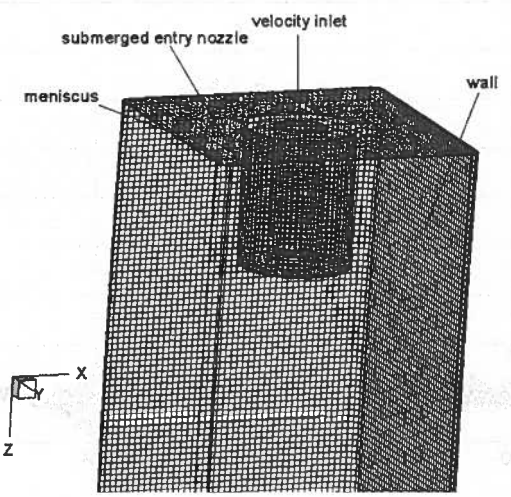

Fig. 4. The computational grid in the upper part of the object

The computational grid composed of 541178 control volumes was generated in the Gambit preprocessor. Figure 6 shows the upper zone of the mould with the descriptions of some boundary conditions, covering part of the tundish entry nozzle submerged in the liquid steel. For solving the system of differential equations of the model employed, for transient conditions with a time step from 0.001 to 0.01 s, the commercial program Fluent was used. An Intel Pentium IV 3.0 GHz computation unit was used, with the computation time amounting to approximately 860 hours.

6. Computation results

As a result of numerical computations carried out, the solution of the system of equations of the applied mathematical model was obtained, thanks to which it was possible to make a map of the distribution of fields of velocities, intensities of liquid steel turbulence in the slab longitudinal section plane passing through the centre of the submerged entry nozzle, temperature variations, as well as the front of crystallization in the solidifying continuous square cross-section slab.

Similarly as for the test object, Figure 5 discloses the occurrence of dead zones. With the passage of time, the intensity of liquid steel stirring in particular volumes of the continuous slab increases, the evidence of which is a considerable increase in velocity. The presented velocity fields and turbulence intensity maps (Fig. 6) after 35 seconds from the moment of starting the filling of the casting mould are reflected in the liquid phase fraction in the transverse slab planes (Fig. 8). The intensive steel stream flowing into the mould transfers the heat to the lower part of the continuous slab. Below the mid-height of the object the stream intensity gradually decreases, and the liquid phase successively disappears.

It follows from Figure 7 that the greatest temperature gradients occur at the slab corners and in the central part of the wall at its mid-height on the inner radius.

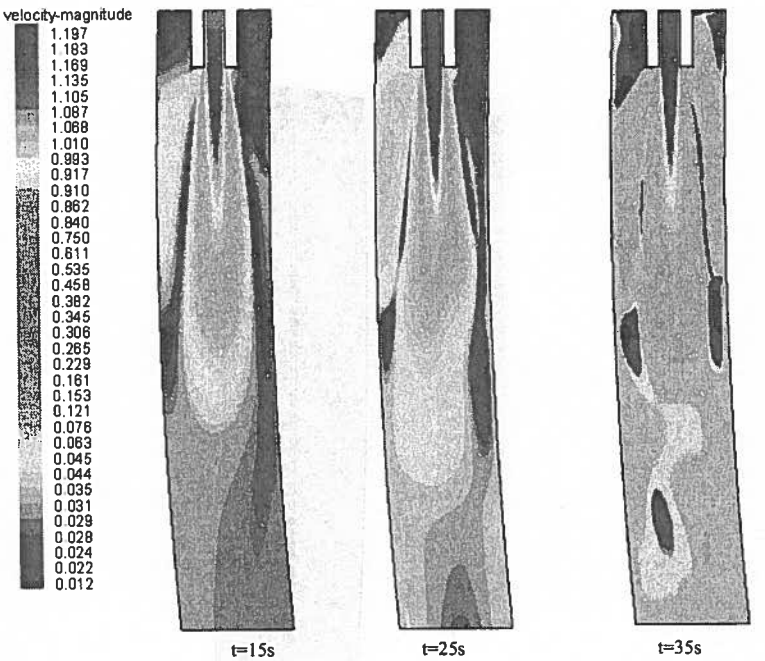

Fig. 5. Liquid steel velocity fields in the longitudinal plane passing through the slab centre

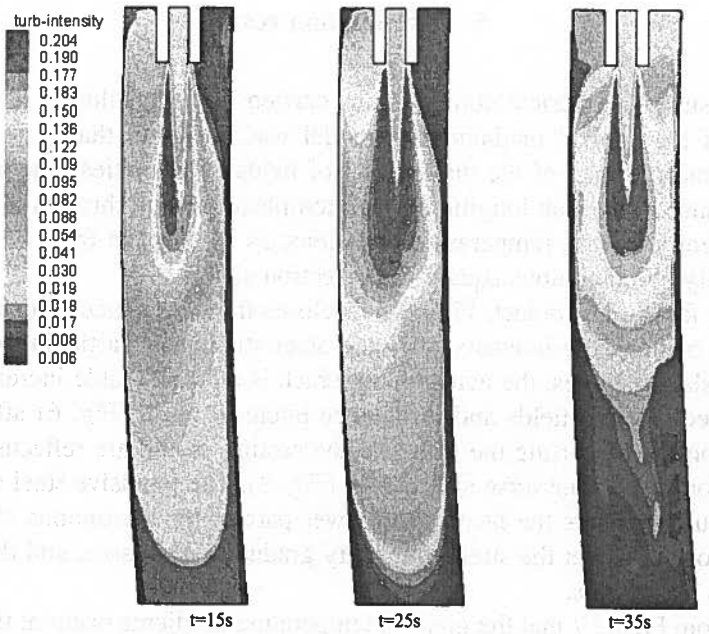

Fig. 6. Liquid steel turbulence intensity fields in the longitudinal plane passing through the slab centre

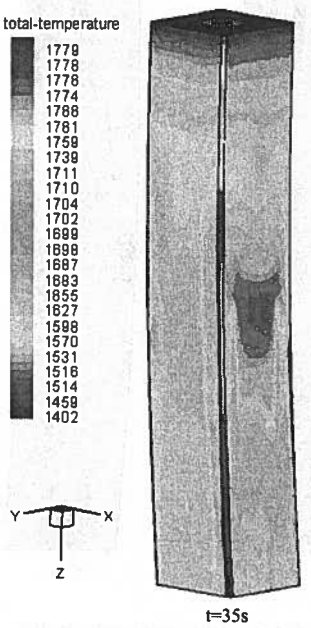

Fig. 7. Temperature fields in the continuous slab

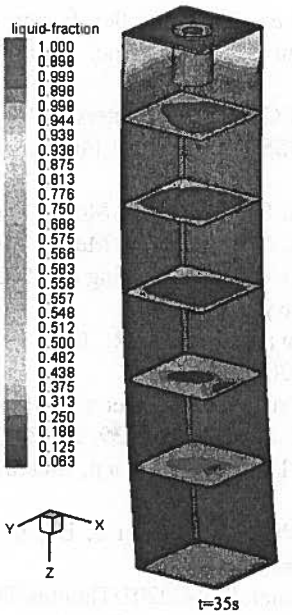

Fig. 8. distribution of liquid phase fraction in the transverse planes

7. Summary

Simulations of the steel solidification process carried out on the test object has made it possible to select an optimal computational grid topology for the entire facility. Moreover, the analysis of the results represented graphically, obtained from numerical modeling, has been confirmed both for the test object and for the whole facility regardless the method of casting mould filling by either open or submerged stream. The occurrence of dead zones in the continuous slab results from the lack of influence of the electromagnetic field produced by the stirrer.

The investigation results reflect the behaviour of liquid steel stream flow in the solidifying continuous slab and constitute a starting material for conducting and improving further computations associated with the computer simulation of the continuous steel casting and solidification process.

REFERENCES

[1] X.K. Lan, J.M. Khodadadi, Int. Journal of Heat and Mass Transfer **44**, 953 (2001).
[2] M. Gonzalez, M.B. Goldschmit, A.P. Assanelli *et al.*, Metall. and ater. Trans. B **34**, 455, (2003).
[3] Y. Meng, B.G. Thomas, Metall. and Mater. Trans. B **34**, 707 (2003).
[4] Y. Meng, B.G. Thomas, Metall. and Mater. Trans. B **34**, 685 (2003).

[5] S. Yokoya, S. Takagi *et al.*., Mater. Sci. Forum **426-432**, 1113, (2003).
[6] B.G. Thomas, Electric Furnace Conf. Proc. 59, ISS, Warrendale, PA, (Phoenix, AZ), **3**, (2001).
[7] L. Beitelman, Effects of Casting Parameters on Stirring Flow Velocity and Control in Continuous Casting Molds, ISS 60th Electric Furnace Conf. in San Antonio, Texas, Nov. 2002.
[8] Q. Yuan, B.G. Thomas, S.P. Vanka, Metall. and Mater. Trans. B **35**, 685 (2004).
[9] Q. Yuan, B.G. Thomas, S.P. Vanka, Metall. and Mater. Trans. B **35**, 685 (2004).
[10] B.G. Thomas, S.P. Vanka, Manufacturing and Industrial Innovation Research Conf., San Juan, Puerto Rico, January 7-10 (2002).
[11] H.J. Odenthal, I. Lemanowicz, R. Gorissen, H. Pfeifer, Metall. and Materials Trans. B **33**, 163 (2002).
[12] D.T. Creech, B.G. Thomas, CFX User's Conf. Wilmington, DE, Oct. 1 (1998).
[13] A.K. Tieu, I.S. Kim, Int. J. Mech. Sci. **39**, 2, 185 (1997).
[14] F.C. Chang, J.R. Hull, L. Beitelman, Metall. and Materials Trans. B **35**, 1129 (2004).
[15] L. Zhang, S. Yang, X. Wang, K. Cai, J. Li, X. Wan, B.G. Thomas, AISTech 2004 Proceedings **2**, 879 (2004).
[16] http://www.tms.org/pubs/journals/JOM/0201/Thomas/Thomas-0201.html
[17] S. Wang, S. Louhenkilpi, P. Hooli, J. Vatanen, AISTech 2004 Proceedings **2**, 361 (2004).
[18] M. Kamal, Y. Sahai, AISTech 2004 Proceedings **2**, 681 (2004).
[19] B. Li, T. Okane, T. Umeda, Metall. and Materials Trans. B **31**, 1149 (2000).
[20] B. Li, T. Okane, T. Umeda, Metall. and Materials Trans. B **32**, 1053 (2001).
[21] R.M. Mc David, B.G. Thomas, Metall. and Materials Trans. B **27**, 672 (1996).
[22] C.R. Swaminathan, V.R. Voller, Metal. Trans. B **23**, October, 651 (1992).
[23] V.R. Voller, C.R. Swaminathan, Numer. Heat Transfer B **19(2)**, 175 (1991).
[24] FLUENT User's Guide, Fluent Inc. 1998.
[25] C.A Santos, J.A. Spim, A. Garcia, Engineering Applications of Artificial Intelligence **16**, 511 (2003).
[26] J.K. Park, B.G. Thomas, I.V. Samarasekera, Ironmaking and Steelmaking **29**, 5, 359 (2002).
[27] B. Lally, L. Biegler, H. Henein, Metal. Trans. B 21, August, 761 (1990).
[28] X.K. Lan, J.M. Khodadadi, Int. Journal of Heat and Mass Transfer, 44, 953 (2001).
[29] K. Okamura, H. Kawashima, The Sumitomo Search, No. 45, March, 9 (1991).
[30] I. Staniewski, W. Derda, J. Jowsa, VI Międzynarodowa Konferencja Naukowa - Nowe Technologie i Osiągnięcia w Metalurgii i Inżynierii Materiałowej, Częstochowa, 48 (2004).
[31] J. Savage, W.H. Pritchard, Journal of Iron and Steel Institute, 269 (1954).
[32] M. Gonzalez, M.B. Goldschmit, A.P. Assanelli *et al.*., Metallurgical and Materials Trans. B **34**, 455 (2003).
[33] R.I.L. Guthrie, T. Emi, Materials Trans., JIM **37**, 3, 540 (1996).

Received: 10 May 2005.